

Alma Mater Studiorum Università di Bologna  
Archivio istituzionale della ricerca

A Low-Cost System for Quick Measurements on Noise Barriers in Situ

This is the final peer-reviewed author's accepted manuscript (postprint) of the following publication:

*Published Version:*

Guidorzi P., Garai M. (2022). A Low-Cost System for Quick Measurements on Noise Barriers in Situ. IEEE TRANSACTIONS ON INSTRUMENTATION AND MEASUREMENT, 71, 1-14 [10.1109/TIM.2022.3218037].

*Availability:*

This version is available at: <https://hdl.handle.net/11585/904358> since: 2023-11-24

*Published:*

DOI: <http://doi.org/10.1109/TIM.2022.3218037>

*Terms of use:*

Some rights reserved. The terms and conditions for the reuse of this version of the manuscript are specified in the publishing policy. For all terms of use and more information see the publisher's website.

This item was downloaded from IRIS Università di Bologna (<https://cris.unibo.it/>).  
When citing, please refer to the published version.

(Article begins on next page)

This is the final peer-reviewed accepted manuscript of:

**P. Guidorzi and M. Garai, "A Low-Cost System for Quick Measurements on Noise Barriers in Situ," in IEEE Transactions on Instrumentation and Measurement, vol. 71, pp. 1-14, 2022, Art no. 6503714**

The final published version is available online at:

<https://doi.org/10.1109/TIM.2022.3218037>

#### Terms of use:

Some rights reserved. The terms and conditions for the reuse of this version of the manuscript are specified in the publishing policy. For all terms of use and more information see the publisher's website.

*This item was downloaded from IRIS Università di Bologna (<https://cris.unibo.it/>)*

***When citing, please refer to the published version.***

# A Low-Cost System for Quick Measurements on Noise Barriers in Situ

Paolo Guidorzi, Massimo Garai

**Abstract**— This paper describes the development of a low-cost device for measuring the acoustic intrinsic characteristics of noise barriers. The system is based on the Teensy 4.1 microcontroller combined with a few other components. The measurements are carried out using a vertical linear microphone antenna housing 6 microphones and a lightweight loudspeaker, wireless connected to the main unit. Both the main system unit and the amplified loudspeaker are powered from normal 5 V USB battery packs, which are easily rechargeable and interchangeable. The system measures 6 impulse responses using an MLS signal and performs a series of calculations and frequency analyses to characterize the device under test, following a simplified version of the European standards EN 1793-5 and EN 1793-6 (commonly referred to as the 'Adrienne method'). One measurement takes few minutes, obtaining results comparable to those obtained with the Adrienne method, which requires a more complicated and heavy measuring equipment and is much more expensive and time consuming.

**Index Terms** — noise barrier, acoustic measurement, low-cost instrumentation, Teensy microcontroller, signal processing, EN 1793-5, EN 1793-6.

## I. INTRODUCTION

THE measurement of the acoustic intrinsic characteristics of noise barriers, i.e. airborne sound insulation and sound absorption, has become increasingly important in recent years. Some decades ago, only laboratory measurements on samples purposely built inside reverberation rooms were possible; however, the diffuse sound field created in these rooms is very dissimilar from the sound field propagating from the traffic source to a freestanding noise barrier outdoors. In situ measurements on installed noise barriers became a reality with the advent of the European standards EN 1793-5 and EN 1793-6 (known as the *Adrienne method*) [1]-[2]. These standards have the advantage of measuring the quality of the actual noise barrier, including workmanship, not an artificial laboratory sample. Nowadays these measuring methods are routinely applied in many European countries: i) in test fields nearby the factory, prior to marketing, to check a new product; ii) at the installation site, along highways and railways, in order to assess the barrier's effective performance, to check for possible installation errors and non-conformity with specifications; iii) repeatedly over time at the installation site, to check the performance decay over the years.

EN 1793-5 and EN 1793-6 measurement system, visible in Figure 3 (a) or in Figure 17 (a), require the use of a square grid with 9 microphones, spaced 0.4 m apart, an artificial sound source (both held at a height of 2 m from the ground) and a measurement and processing unit - usually a portable computer - a multi-channel audio interface, a specific software package and various other accessories such as speaker power amplifier,

cables, microphone preamplifiers and a portable 220 V power source for all instrumentation (motor-driven generator or high-capacity batteries and inverter).

The measurement system equipment prescribed by European standards EN 1793-5 and EN 1793-6 is expensive and heavy to transport and takes some time to assemble and disassemble in the field (the side of a highway or railroad, usually left open to traffic during the test). Therefore, the need arose to create a lightweight, low-cost measurement system that could quickly and reliably provide results comparable to those of the standard system.

Today it is common to use small measurement systems based on microcontrollers, created for a specific task, with portability and flexibility features. These low-cost, special-purpose systems are being created and used in a wide variety of research and application fields, such as Acoustics and Electroacoustics measurements [3]-[9], Electrochemical biosensors [10]-[11], Electrochemical impedance spectroscopy [12], Electronics [13]-[18], Environmental measurements [19]-[24], Medical [25], Micro-electromechanical [26], Micro-fluidics [27], Optical particle counters [28], low distortion Sine-wave generation [29], Soil moisture measurement [30]-[31] and Yeast concentration measurement for brewery [32].

In this paper, a low-cost acoustic noise barriers measurement system based on the Teensy development board is presented [5]-[7], [9], [12], [16], [27], [28] and [31].

## II. PRINCIPLE OF THE METHOD

In order to obtain measurement results comparable with the European standard, the principles of the measurement method used in the new portable system are the same, but instead of a square grid of 9 microphones, visible in Figure 3 (a) or Figure 17 (a), a vertical microphone antenna, visible in Figure 3 (b) or Figure 17 (b), is used, on which 6 microphones are installed. The microphones on the vertical antenna are spaced 0.40 m apart and positioned at a height from ground from 1.20 m up to 3.20 m. The measurement method described below can therefore be applied using either the square grid or the linear antenna, by setting the correct value to the geometric divergence correction coefficient  $C_{geo,k}$  in formula (1), depending on the relative distances between loudspeaker, microphones and barrier. In the following, the vertical antenna method, outlined in Figures 1 and 2, is illustrated.

### A. Sound absorption

The European methodology assesses indirectly sound absorption by measuring sound reflection, its complementary characteristics. The sound source (loudspeaker) produces an

acoustic signal that first reaches the microphone antenna or grid, then the surface of the barrier, and finally is reflected from it and reaches the microphone antenna or grid again (Figure 1 (a)). Each microphone, being placed between the sound source and the device under examination, receives the direct sound pressure wave travelling from the sound source to the device under examination, as well as the reflected sound pressure wave (including scattering) by the device under examination. The direct sound pressure wave can best be acquired with a separate free-field measurement maintaining the same sound source and microphone antenna or grid geometric configuration but in the absence of the noise barrier (Figure 1 (b)). The ratio of the power spectrum of the reflected components over the power spectrum of the direct components makes it possible to calculate the sound reflection index. This quantity is defined in each one-third octave band, averaging data from all the microphone positions, as [1], [42]:

$$RI_j = \frac{1}{n_j} \sum_{k=1}^{n_j} \left[ \frac{\int_{\Delta f_j} |F[h_{r,k}(t) \cdot w_{r,k}(t)]|^2 df}{\int_{\Delta f_j} |F[h_{i,k}(t) \cdot w_{i,k}(t)]|^2 df} \cdot C_{geo,k} \cdot C_{dir,k}(\Delta f_j) \cdot C_{gain,k}(\Delta f_g) \right] \quad (1)$$

where:

- $h_{i,k}(t)$  is the incoming free-field reference impulse response component from the  $k$ -th microphone
- $h_{r,k}(t)$  is the reflected impulse response component, at the  $k$ -th microphone
- $w_{i,k}(t)$  is the *Adrienne* time window [1] for the incident reference component of the free-field impulse response, at the  $k$ -th microphone
- $w_{r,k}(t)$  is the *Adrienne* time window for the reflected component, at the  $k$ -th microphone
- $F$  is the symbol for the FFT operator
- $j$  is the index of the 1/3 octave frequency bands, from 100 Hz to 5 kHz
- $\Delta f_j$  is the width of the  $j$ -th 1/3 octave frequency band
- $k$  is the number of the microphone, from 1 to 6 or 9
- $n_j$  is the microphone position number to average over
- $C_{geo,k}$  is a geometrical divergence correction factor, to compensate the direct and reflected waves path difference, at  $k$ -th microphone
- $C_{dir,k}(\Delta f_j)$  is a loudspeaker directivity correction factor, at the  $k$ -th microphone
- $C_{gain,k}(\Delta f_j)$  is a gain mismatch correction factor, used to correct errors in amplification settings between the free-field and barrier measurements, if required, at the  $k$ -th microphone

To obtain local information of the barrier behaviour, the reflection index coefficients from individual microphones can be analysed instead of the average value.

#### B. Airborne sound insulation

The sound source (loudspeaker) produces an acoustic signal

that travels across the noise barrier and is in part reflected, in part transmitted and in part diffracted by it. The microphone placed on the other side of the device under test receives both the transmitted sound pressure wave travelling from the sound source through the device under test, and the sound pressure wave diffracted by the top edge of the device under test (Figure 2 (a)). If the measurement is repeated without the device under test between the loudspeaker and the microphone, the direct free-field wave can be acquired (Figure 2 (b)). The ratio of the power spectrum of the transmitted component over the power spectrum of the direct component makes it possible to calculate the sound insulation index.

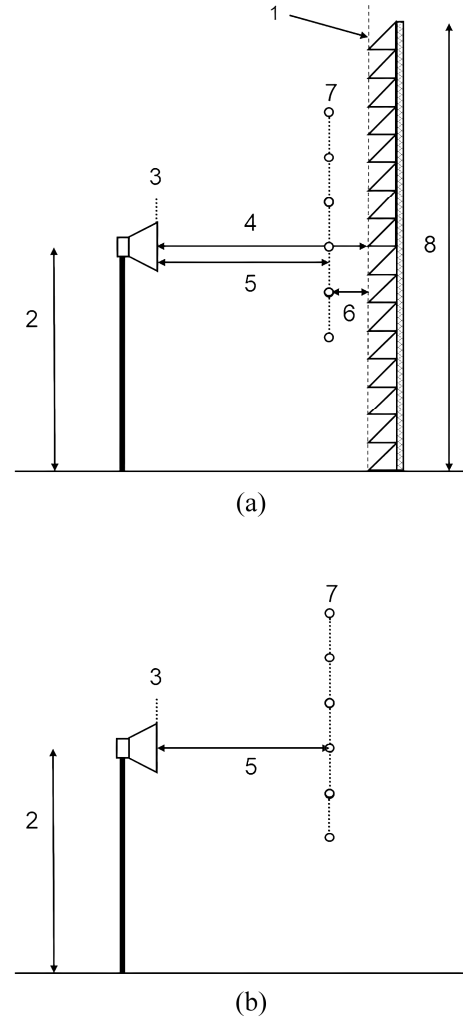


**Figure 1.** (not to scale) Sketch of the sound source and the microphone antenna in place for measuring the sound reflection index. (a): in front of the road traffic noise reducing device under test for sound insulation index measurements. (b): in the free field. 1: Sound source reference surface. 2: Reference height  $h_S = 2$  m. 3: Loudspeaker front panel. 4: Distance between the loudspeaker front panel and the reference surface,  $d_S = 1.5$  m. 5: Microphone reference surface. 6: Distance between the microphone antenna and the mic. reference surface,  $d_M = 0.25$  m. 7: Microphone antenna. 8: Noise barrier height,  $h_B$  [m].

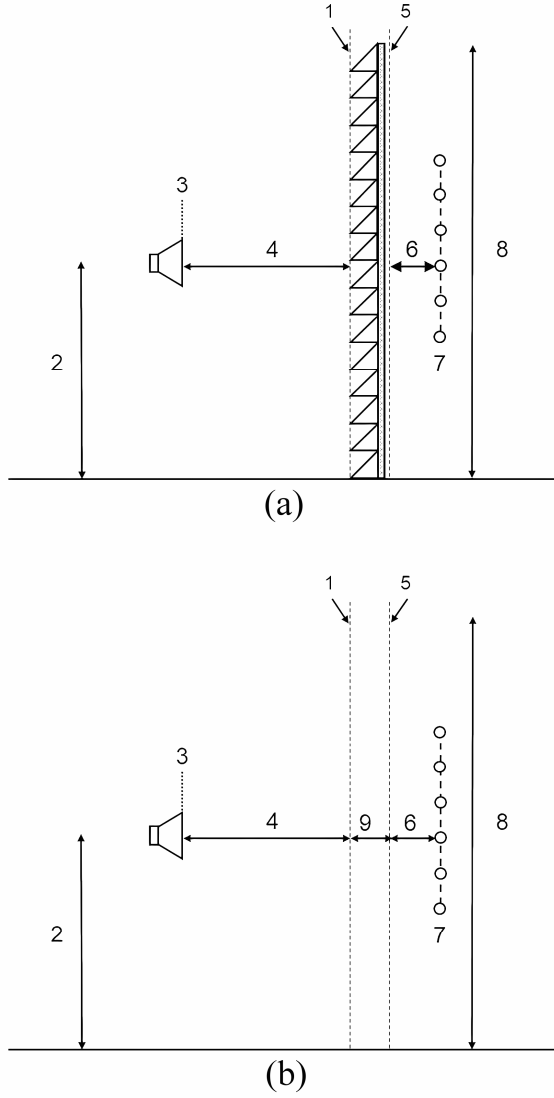


**Figure 2.** (not to scale) Sketch of the sound source and the microphone antenna in place for measuring the sound insulation index. (a): in front of the road traffic noise reducing device under test for sound insulation index measurements. (b): in the free field. 1: Sound source reference surface. 2: Reference height  $h_S = 2$  m. 3: Loudspeaker front panel. 4: Distance between the loudspeaker front panel and the reference surface,  $d_S = 1$  m. 5: Microphone reference surface. 6: Distance between the microphone antenna and the mic. reference surface,  $d_M = 0.25$  m. 7: Microphone antenna. 8: Noise barrier height,  $h_B$  [m].

This quantity is defined in each one-third octave band as [2], [42]:

$$SI_j = -10 \cdot \log_{10} \left\{ \frac{1}{n} \sum_{k=1}^n \frac{\int_{\Delta f_j} |F[h_{i,k}(t)w_{t,k}(t)]|^2 df}{\int_{\Delta f_j} |F[h_{i,k}(t)w_{i,k}(t)]|^2 df} \right\} \text{ dB} \quad (2)$$

where:

- $h_{i,k}(t)$  is the incoming free-field reference impulse response component from the  $k$ -th microphone
- $h_{t,k}(t)$  is the transmitted impulse response component, at the  $k$ -th microphone
- $F$  is the symbol for the FFT operator
- $k$  is the number of the microphone, from 1 to 6 or 9
- $j$  is the index of the 1/3 octave frequency bands, from 100 Hz to 5 kHz
- $\Delta f_j$  is the width of the  $j$ -th 1/3 octave frequency band
- $w_{i,k}(t)$  is the *Adrienne* time window for the incoming free-field reference impulse response component from the  $k$ -th microphone
- $w_{t,k}(t)$  is the *Adrienne* time window for the transmitted component, at the  $k$ -th microphone
- $n$  = the number of microphones on the grid or antenna

To obtain local information of the barrier behaviour, the sound insulation index from individual microphones can be analysed instead of the average value.

### III. SIGNAL PROCESSING

In both cases 6 or 9 impulse responses are acquired close to the noise barrier under test, one for each microphone on the linear antenna or on the square grid, by means of the well-known MLS (Maximum Length Sequence) technique, applied to many branches of acoustics since many years [33]-[40]. Next, other 6 or 9 free-field impulse responses are measured, placing loudspeaker and microphone grid away from the noise barrier and other obstacles but keeping the same relative distances.

For calculating  $RI$ , the measured free-field impulse responses are used for the subtraction in the time domain of the part of the direct signal that contaminates the reflected part of measurements in front of the barrier [41]. The reflected and free-field parts of each of the 6 or 9 impulse responses are then windowed and Fourier-transformed into third-octave band spectra. From the ratio of the reflected and direct spectra, with the appropriate weighting and compensation as per formula (1), the sound reflection index is obtained.

A similar procedure, again in two steps, is carried out to measure the sound insulation characteristics of the noise barrier. In the free-field measurements, the thickness of the barrier must be taken into account when positioning the microphone grid at the correct distance from the loudspeaker. The ratio between the spectra of the windowed signal transmitted by the barrier and those in the free field, appropriately weighted and averaged as per formula (2), gives the sound insulation index ~~is obtained~~.

It should be noted that the measurement geometry determines the maximum time width of the data analysis window, in order to avoid spurious reflections from nearby surfaces – including ground – when measuring sound reflection or sound passing over the barrier, when measuring sound insulation. The European standards, with reference to the square grid, set the time width of the analysis window at 7.9 ms (upper two microphone rows) or 6.0 ms (lower microphone row) and this consequently determines the lower frequency

limit in the spectral analysis; for a 4 m high noise barrier under normal conditions, valid data in the 1/3 octave bands from 200 Hz to 5 kHz are obtained.

#### IV. ADRIENNE AND QS EQUIPMENTS

The Adrienne measurement system made in the DIN laboratory, shown in Figure 3 (a), consists of a laptop computer, an external RME Madiface XT audio interface connected via a coaxial cable to a 16-channel Analog to MADI/ADAT converter RME M-16 AD. The microphones are Piezotronics PCB model 130F20, together with dedicated preamplifiers. The sound source is a Zircon by Acoustics Engineering, amplified with a Samson Servo 201A power amplifier. The microphone grid was built for this system, and a custom software runs on the computer for real-time measurement and calculation of the barrier parameters, as described in [1], [2]. This system is very accurate and provides highly repeatable results, as confirmed by a European inter-laboratory test in which our laboratory participated in 2012 [42]. Measurement systems like this are used to check the conformity with specifications of installed noise barriers. On the other hand, computer, amplifiers and other system components require mains 220 V power supply (from 12 V batteries with inverter or from a motor-driven generator set); they are heavy and the complete system requires some time for assembly and disassembly at the measuring site (motorway or railway with traffic flow) and must be operated by expert users. As a consequence, the conformity of expensive works is evaluated on the basis of very few tests. Extensive tests for maintenance purposes are not possible. A more fast and agile measuring system would be required instead, to do dozens of tests in one day. It should be used by every operator after a short training.

In order to answer to this need, a new complete system for measuring on noise barriers has been designed (see Figure 3 (b)) with the following goals:

- be a quick method, to be applied in situ;
- be effective for both sound insulation and sound absorption measurements;
- be lightweight and easy to carry on site;
- use an easy-to-handle microphone antenna; a linear one is preferable instead of a square grid;
- be low-cost;
- run on rechargeable batteries (USB / 5 V) with a long operating autonomy;
- have wireless audio signal transmission to the loudspeaker;
- be easy-to-use by non-expert users, e.g., performing a measurement cycle pushing only few buttons;
- give measurement results comparable to Adrienne system;
- calculate and display results at the measurement site;
- save and export measurements and results to PC.

All these goals were achieved with the system described in the following, called Quick System (QS), operated by a Teensy 4.1 development board, based on ARM Cortex-M7 micro-

controller, running at 600 MHz. In Figure 3 (b) an early prototype of the QS is shown, compared with the *official* Adrienne measurement system, shown in Figure 3 (a), during a comparison test on the same noise-barrier site, along the A22 motorway, near Isera, Italy.

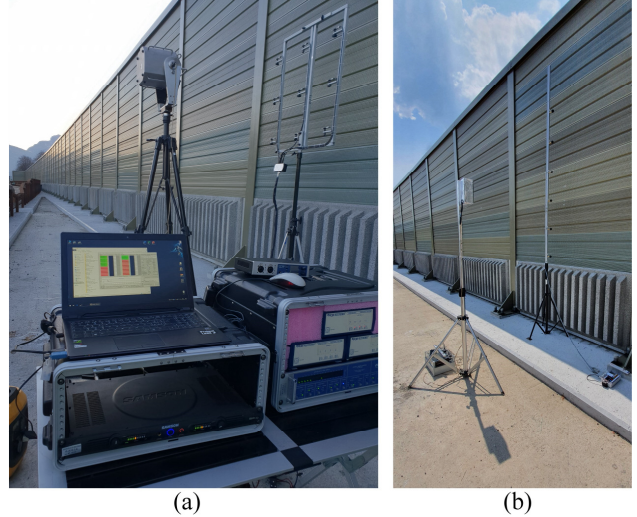


**Figure 3.** (a) Adrienne measurement system; (b) the early prototype of the Quick System. Same test site alongside the A22 motorway.

#### V. QUICK SYSTEM DESIGN

The new Quick System uses a Teensy 4.1 board as its main control unit, to which 16 MB of RAM memory (soldered into the rear face) were added in order to easily perform calculation and signal processing operations, especially the FHT (Fast Hadamard Transform) on blocks of 256K floating point samples and the FFT (Fast Fourier Transform) for calculations according to formulas (1) and (2).

The Teensy board has proved to have sufficient computing power and memory resources to be used in real-time audio applications requiring advanced signal processing [49]-[50].

For measuring the impulse responses prescribed by the standards [1]-[2], the MLS signal was chosen over other ones, such as the ESS (Exponential Swept Sine), because the MLS signal has been found to be more robust against strong background noise (flowing traffic) for noise barriers measurement applications [43]-[44] and requires less computational resources for the reconstruction of the impulse response, thanks to the FHT algorithm [33]-[34], [39]-[40].

Figure 4 shows the block diagram of the entire Quick System, consisting of the following elements:

- linear antenna with 6 microphones;
- lightweight loudspeaker;
- wireless signal transmission system;
- main control unit.



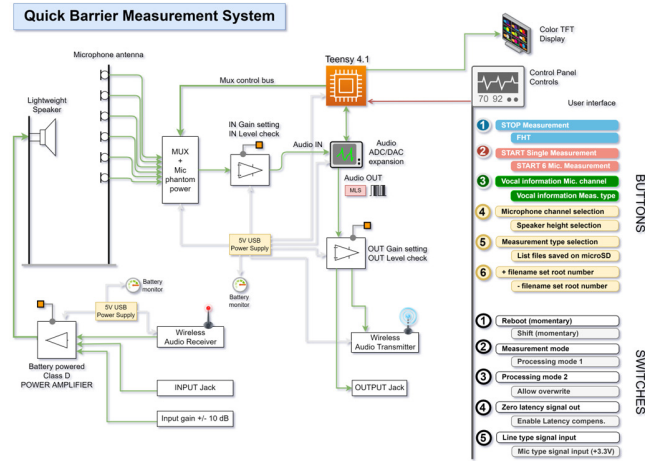


**Figure 4.** Block diagram of the Quick System.

#### A. Microphone linear antenna

Positioning the Adrienne square grid exactly parallel to the plane of reference of the noise barrier has proven to be time consuming on an irregular terrain, due to the two possible rotations on the vertical and horizontal planes. Therefore, a vertical antenna has been preferred for the QS. Moreover, moving it in the horizontal direction a complete scan of the tested barrier is easily obtained (see Section VIII.D and Figure 22).

The vertical linear antenna houses 6 microphones, spaced 0.4 m apart, at a height above ground of 1.20 m, 1.60 m, 2.00 m, 2.40 m, 2.80 m, 3.20 m and labeled as M1 to M6, from bottom to top. Each microphone is made up of a CMA-4544 omnidirectional electret capsule, powered from the QS main unit (3.3 V phantom voltage) and mounted on a standard RCA plug. The six microphones are directly connected with a multi-core wire to the QS main unit, as shown in Figure 5 (a) and (c).

#### B. Lightweight loudspeaker

The lightweight loudspeaker, shown in Figure 5 (d), consists of a low-profile box (0.25 m x 0.25 m x 0.1 m) on which a Sica Z002601 loudspeaker (120 W, 8  $\Omega$ ) is mounted, connected to a class D power amplifier model ST CCA044V1, fitted in a box on the support stand, shown in Figure 5 (b). Outside the box there is an USB battery pack that powers the amplifier (via a step-up circuit to raise 5 V to 15 V) and recharges the wireless receiver if necessary. Optionally, it is possible to connect the audio signal to the amplifier via cable.

The battery pack used is 20100 mAh / 74.37 Wh. The power amplifier draws about 1 W when idle and about 10 W during MLS signal output, so a battery charge lasts several working days on average.

#### C. Wireless signal transmission system

The MLS test signal, generated by the main unit, can be sent to the loudspeaker in two ways: either directly via cable or using a wireless digital transmitter and receiver operating at 2.4 GHz. The wireless system used is the Andoer MX5 2.4G, which

transmits uncompressed audio digitized at 48 kHz, 16 bits. There is a switch in the QS control panel that enables or disables software compensation for the fixed latency introduced by the digital wireless system. The wireless digital transmission of the signal to the loudspeaker is particularly useful when measuring sound insulation and the microphone antenna and the loudspeaker are placed on opposite sides of the noise barrier (Figure 2). In the Adrienne system, the problem was solved by sending digitally the audio signals over a coaxial cable, using the MADI audio standard; this was an expensive and impractical solution - although reliable - as it is always necessary to run a long coaxial cable from one side of the noise barrier to the other, for example passing it over the top.

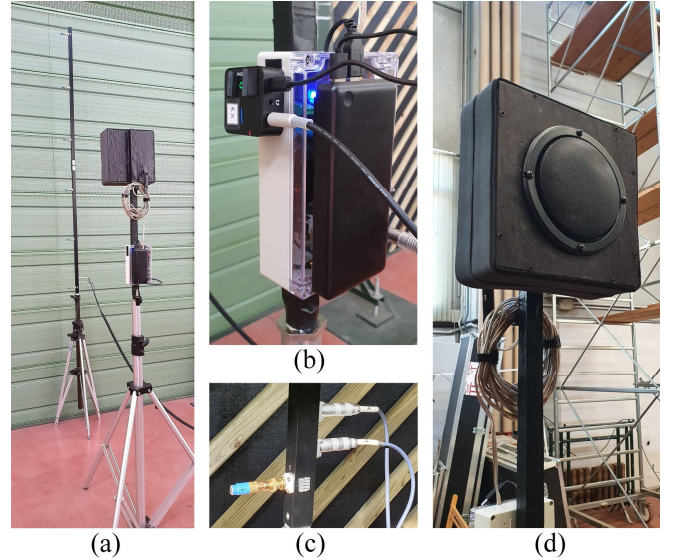


**Figure 5.** (a) Microphone antenna and loudspeaker; (b) battery powered loudspeaker amplifier and wireless receiver; (c) microphone mounted on the vertical linear antenna; (d) lightweight loudspeaker.

## VI. MAIN CONTROL UNIT

#### A. Hardware design

The main control unit employs a Teensy 4.1 development board, expanded with 16 MB RAM. The following additional components are also used: a Teensy audio board Rev. D (SGTL5000 chipset), a CD74HC4067 16-channels multiplexer, a 240 x 320 pixels color TFT display and other auxiliary components such as voltage regulators, buttons and switches. Figure 6 and Figure 7 show the circuit schematic diagram and the PCB.

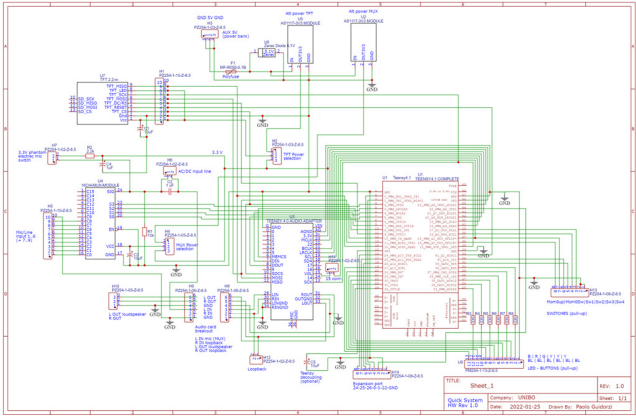


Figure 6. Main unit schematic diagram.

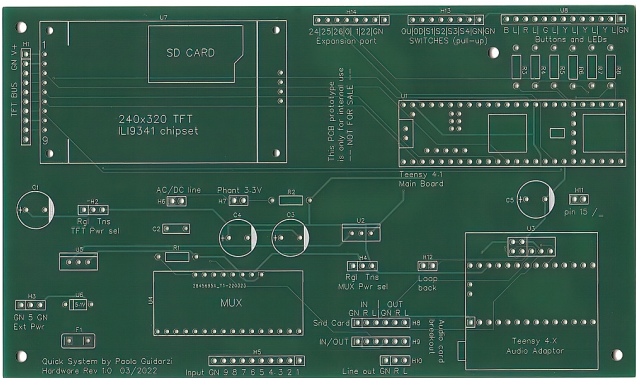


Figure 7. Printed Circuit Board.

A 3.3 V Phantom power for the CMA-4544 electret capsules is supplied directly from the main unit, via a 2.2 k $\Omega$  resistor. If an external preamplifier or another type of microphone is used, phantom power can be disabled with a switch on the panel.

Finally, in the circuit there is a TFT display connected to the Teensy board by the SPI bus.

The audio board has 2 input channels and 2 output channels (44.1 kHz, 16 bit) whereas there are 6 microphones on the antenna; a multiplexer was therefore used to sample the audio signal coming from the 6 microphones one after the other using one of the 2 input channels, while the MLS signal is delivered to one of the 2 output channels, then sent to the loudspeaker via the wireless transmitter. The second output channel is instead permanently looped back to the second input channel for two purposes: the first is to measure the latency of the digital audio system (the delay in samples between the input signal and the output due to the converters and the software), which will be used to correctly time align the impulse response reconstructed from the sampled signal (thanks to the properties of the MLS signal [33]-[34]); furthermore, the signal generated on the second channel includes some pulses used as markers to verify that no data loss occurs in the sampling process (as the two channels are always sampled synchronously); multiple checks on the measured data, including their amplitude, both in the microphone channel and in the loopback channel, are carried out and if any error is detected the software will automatically repeat the measurement.

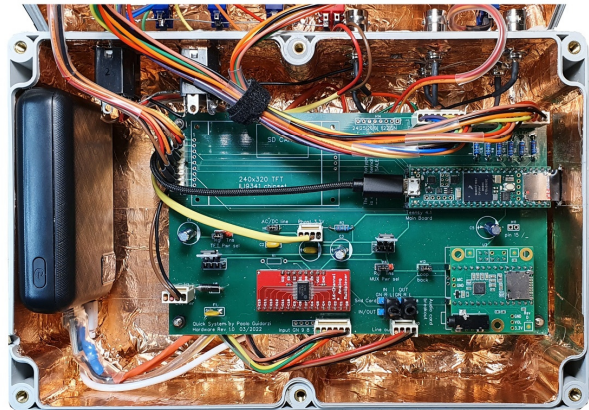
The extra latency is not added to the calculation if zero latency is set in the device panel with the appropriate switch, when the loudspeaker is connected via a cable.

Inside the container there is also a 10000 mAh / 37 Wh USB battery pack. The power consumption of the entire QS main unit is about 1.2 W so the working time is around 30 hours and in case of need it is always possible to power the unit from an external USB battery pack.

Figure 8 (b) shows the inside of the enclosure. On the left is visible the battery pack and on the right the main PCB with the electronic components. The inside of the plastic container of the prototype is covered with copper tape to avoid electromagnetic interference. Figure 8 (a) shows the backside of the control panel; on its frontside the TFT display, buttons and switches are housed.



(a)



(b)

Figure 8. (a) Inside the main unit; (b) PCB main board.

Figure 9 (a) shows the main panel of the QS. There are switches for the main options and 6 buttons to start or stop the measurements, select the microphone channel or measurement type and other secondary functions, described in detail in the following. Figure 9 (b) shows the rear panel, where the 6 inputs for the microphone signals and the output for the signal to the loudspeaker are fitted.



### B. User interface and operation

The main goal of the design and ergonomics of the user interface was the easiness of use in order to minimize possible operating errors and make the instrument usable even by non-expert operators.

In the main panel, each button and switch is assigned to a single function or at most two, using SHIFT. To make a measurement, a number must be assigned to the set of data to be measured, using SET+ and SET-, then the type of measurement (Reflection-Barrier, Reflection Free field, Isolation-Barrier, Isolation Free field) must be selected using the MEA.TYP button; a microphone number can be selected with CH.1-6 button for a single measurement shot, or the automatic measurement can be launched for all 6 microphones. In this last case, the software will do 6 measurements, automatically repeating those where errors are found (e.g., due to excessive background noise), will compute the impulse response by means of an FHT of sampled data and will automatically save the results as IEEE floating point WAV files, using filenames identifying set number, type of measurement and microphone position. At the end of the measurement cycle, the 2 switches PROC.1 and PROC.2 can be used to have an instant view of the results and verify the correctness of the measurement and the acoustic performance of the barrier around the 6 microphone positions. The TALK1/TALK2 button when pressed gives synthetic voice indications about the selected measurement type and microphone, which is helpful when the system is used in bright sunlight and the display is difficult to read.

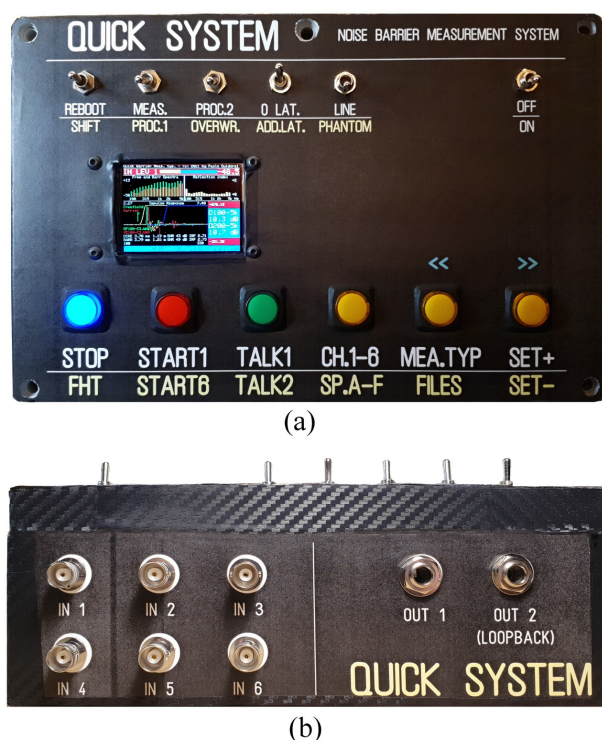


Figure 9. (a) Front panel; (b) rear panel.

Figure 10 (a) shows an example of sound insulation calculation made on board of the QS control unit from data measured at microphone 4. On the display are visible: at the bottom, the file name; just above, a plot with the initial part of the measured impulse responses (in green the free-field one and in red the noise barrier one, rescaled in amplitude) and the *Adrienne* data selection window (in violet) [2], positioned equally on the time axis for both impulse responses. Some other auxiliary data calculated by the software on the impulse responses, such as SNR ratio, whose calculation is described in section VIII, peaks time positions, and others, are shown below the impulse responses and are part of the data used by the software to verify the correctness of the measurement. On the right, with blue background, the sound insulation single-number ratings in dB, calculated according to EN 1793-6 in the ranges 100 Hz-5 kHz and 200 Hz-5 kHz, are shown. These single-number rating is calculated weighting the results, which are function of frequency, with the normalized traffic noise spectrum given in EN 1793-3; this provides an overall indication of the noise barrier performance. Above the impulse responses plot, the dB spectra in third-octave bands of the windowed free-field data (in green), of the windowed close-to-barrier data (in red) and the plot of the sound insulation values, in dB, of the barrier in one-third octave bands (in yellow) are shown. At the top of the display a dBFS real-time input signal level bar of the currently selected microphone is shown.

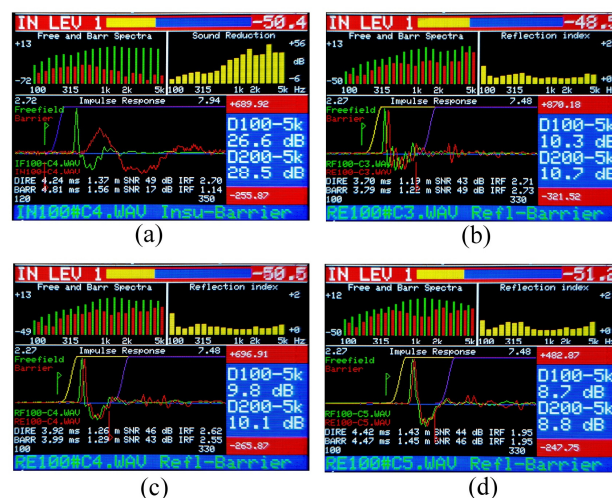


Figure 10. (a) Example of result of sound insulation index measurement at microphone 4; (b), (c), (d) examples of results of sound reflection index measurements at three different microphone positions.

Figure 10 (b), (c) and (d) show examples of the sound reflection calculation, at microphones 3, 4 and 5. Again, the two measured impulse responses are shown, in green the free-field one and in red the reflected one. In this case, the *Adrienne* data windows used to isolate the data for FFT are positioned differently as the sound reflected by the barrier is shifted forward on the time axis compared to the free-field one, due to the longer travel path [1]. As in the previous case, on the right,

on a blue background, the single-number ratings in dB are shown, which provide an overall indication of the sound absorption of the barrier surface (a higher number indicates greater absorption, i.e., better acoustic performance). On the upper left the spectra of the free-field and reflected data are shown, and on the upper right there is the plot of the sound reflection index [1], in third-octave bands, which provides information on how much sound is reflected (lower values indicate less reflection, i.e., better acoustic performance).

It should be noted that in the reflection measurements the initial portions of the free-field and reflected impulse responses are identical and the sound reflected by the barrier (in red) is clearly visible. Identical geometric positioning of the loudspeaker and microphone antenna in the two measurements, free-field and barrier, leads to the best overlap of the initial parts of the impulse responses, but a difference of few samples (fractions of a millisecond) does not appreciably affect the results. In the complete Adrienne system, running on a computer, the two impulse responses are aligned with a least-squares search algorithm, which allows them to be perfectly aligned, within a small fraction of the time sampling step [45], before subtracting the direct response from the reflected one. This operation assures the best result, but involves a very high number of FFTs and IFTs, which is not possible on a microcontroller for computational time reasons. In any case, it has been found in the test measurements that even without this operation the results are very similar to those of the complete Adrienne system (see Section VIII).

The measurement at a single microphone position, using the MLS signal of 256k samples at a sampling frequency of 44.1 kHz (a little less than 6 seconds long), including the time for computation and reconstruction of the impulse response via FHT in memory, takes about 25 seconds. The complete automatic measurement cycle on all 6 microphone positions takes about 2'30". Considering that two set of impulse responses are required for a complete measurement, close to the noise barrier and in the free field, and taking into account also the time for positioning the loudspeaker and microphone antenna, the total time for one measurement of RI or SI in one position is less than 10 minutes.

The free-field measurement (which is basically a reference that is used to normalize the measurement close to the barrier) can also be shared among several close-to-the barrier measurements when the time slot allowed to do measurements alongside a road is short, further cutting the measurement time at several locations close to a long noise barrier.

### C. Software design

The programming of the instrument was carried out in C++ using the Arduino IDE and the Teensyduino plugin [47]. For the audio measurement part, the Teensy Audio System Design Tool, shown in Figure 11, was used; it is a visual programming environment that allows the programming of real-time audio management to be greatly simplified and the generated code to be directly exported for use in the Arduino IDE, ready to be uploaded to the Teensy board [48].

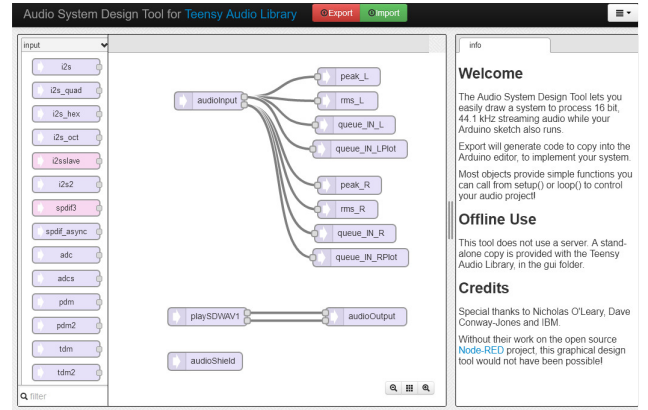


Figure 11. The Teensy online Audio System Design tool.

## VII. DEVICE TESTING AND SPECIFICATIONS

### A. Instrument dynamic range and frequency response

The MLS signal generated by the QS has length 262143 samples, is played by the loudspeaker and then sampled by the microphones. The Fast Hadamard Transform implemented in the software [33], [39]-[40] allows to reconstruct the impulse response of the acoustic system under test in the prescribed cases (free-field, sound reflection on the noise barrier side exposed to traffic or airborne sound insulation across the noise barrier).

Therefore, in order to evaluate the maximum performance of the measurement system alone (without the non-linearities introduced by the loudspeaker and the microphones) a loopback measurement was carried out, connecting with a cable the signal output connector to the signal input connector (and adding an artificial delay otherwise the peak would have been at time zero for automatic latency compensation).

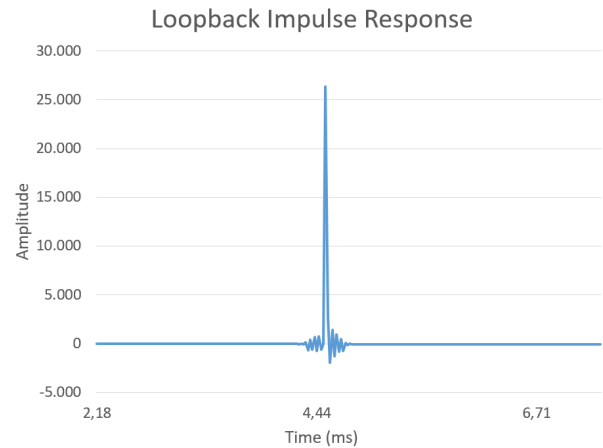


Figure 12. Loopback impulse response of the QS.

Figure 12 shows the loopback impulse response of the system, in practice determined by the combined response of the cascaded DAC and ADC converters and the system's internal audio chain. It should be noted that the scaling of the amplitudes depends on the software reconstruction algorithms and has no

special meaning. Moreover, this amplitude is not calibrated, but this does not matter since the noise barrier acoustic parameters (RI and SI) are always computed as a ratio of components extracted from impulse responses taken with the same equipment and the same setup within a short time.

The impulse responses calculated and saved by QS, as well as all internal calculations, take place on floating point data and the saved WAV files are in PCM 44100 Hz 64 bit IEEE floating point format.

An estimate of the maximum dynamics obtained from the loopback impulse response was calculated by selecting a portion of 20 samples around the peak, where the maximum energy is present, and other 20 samples from the same impulse response data away from the peak, where only background noise is present.

The measured total RMS power of the peak is 78.6 dB while the total RMS power of the noise floor is -5.2 dB, resulting in a signal-to-noise ratio between the maximum peak and the noise floor of 83.8 dB, which is a value quite similar to the ADC specifications of the SGTL5000 codec of 85 dB.

The total lack of spurious peaks over the entire time length of the loopback impulse response indicates the lack of significant distortions in the measurement system [34], [36], [38].

Performing the FFT of the loopback impulse response yields the frequency response of the QS (DAC+ADC), shown in Figure 13, which is sufficiently flat.

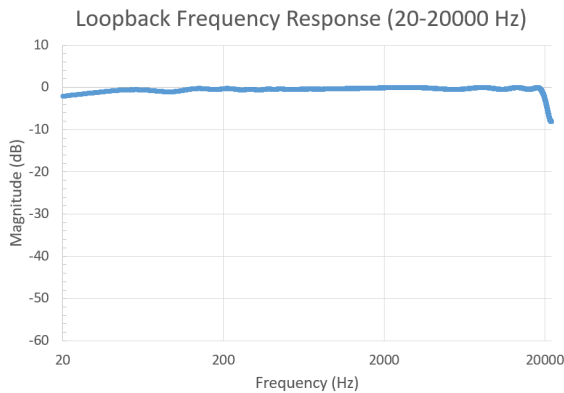


**Figure 13.** Frequency response obtained from FFT of the loopback impulse response of QS.

#### B. Low-cost microphones test

The CMA-4544 electret capsule is a (deliberately) low-cost choice; however, it can provide sufficient performance for this measurement system. From the capsule datasheet it can be seen that the frequency response is reasonably flat in the frequency range 50-10000 Hz (+/- 5 dB). The overall SNR has a specification of 60 dB(A), which is also sufficient for use in this measurement system.

To test the usability of these low-cost electret capsules, a free-field measurement of a loudspeaker box with CMA-4544 microphones and with PCB Piezotronics measurement microphones model 130F20 (used in the Adrienne system) was

carried out. The impulse response of the loudspeaker was measured with both microphones, under the same boundary conditions, and the FFT of the semi-anechoic part was windowed and analyzed, filtering the signal with a pink filter, in order to perform a correct analysis in third-octave bands. Figure 14 shows the one-third octave band spectra obtained from measurements with both microphones. Of course, the responses are not identical but the differences are not too marked and there are no problematic parts in the frequency range prescribed by the European standards (1/3 octave bands from 200 Hz to 5000 Hz).

It should be recalled again that the measurement method described by the European standards always requires the barrier measurement to be normalized with reference to the free-field one, so it is not necessary for the measurement chain to have a flat or perfect response.

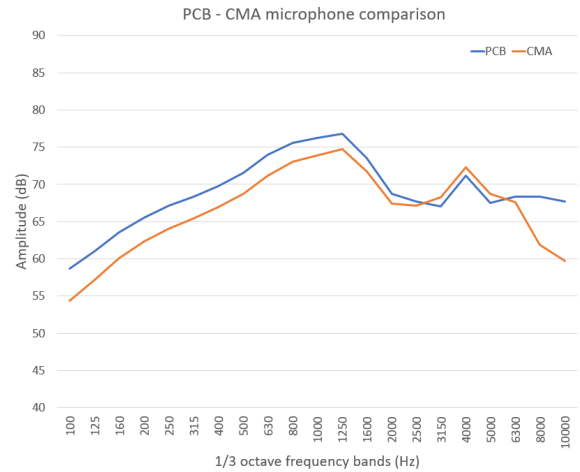


**Figure 14.** Comparison of the PCB Piezotronics model 130F20 microphone with the electret capsule CMA-4544.

#### C. Lightweight loudspeaker test

The lightweight loudspeaker was compared to the Zircon loudspeaker, specifically validated for Adrienne measurements.

The first criterion was the time length of the impulse response of both loudspeakers, which must include most of its energy within the first 3 ms, in order not to contaminate the part of the signal reflected by the barrier. As can be seen from the plots in Figure 15, the lightweight loudspeaker fulfils this specification very well, performing slightly better than the Zircon one.

The second comparison was on frequency response: the response of the two loudspeakers was measured using the same microphone. During the measurement session, wired and wireless signal transmission to the loudspeaker was tested. The results are shown in Figure 16. It can be seen that both loudspeakers perform reasonably well. Moreover, the lightweight loudspeaker as a flatter response at high frequencies, around 5000 Hz. The perfect transparency of the chosen wireless transmitter compared to the wired connection is also noticeable.



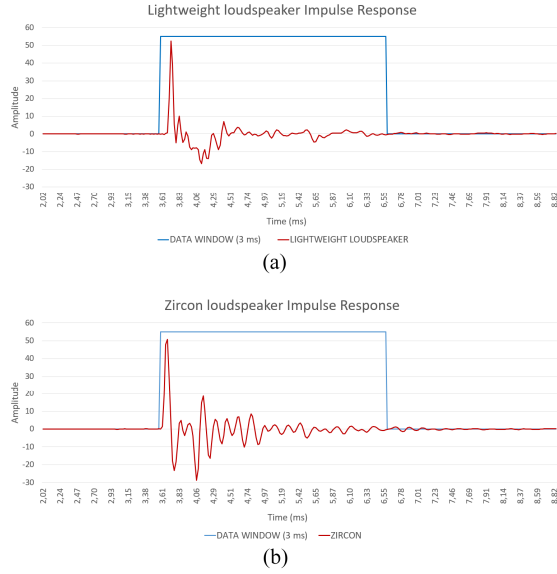


**Figure 15.** Comparison of the free-field impulse responses of the lightweight (a) and Zircon (b) loudspeakers.

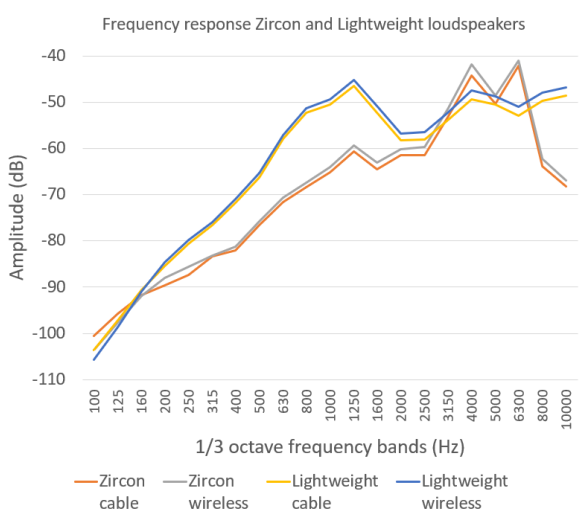


**Figure 16.** Comparison of frequency responses of Zircon and lightweight loudspeakers, with cable and wireless connection.

## VIII. MEASUREMENTS ON NOISE BARRIERS

To be validated, the Quick system was tested on a full-size noise barrier placed in the laboratory. The vertical microphone antenna of Quick System allows to evaluate in a single measurement round the full vertical extension of the barrier, from ground to top (see [46]), but in order to compare the performance of the QS with the already validated Adrienne system, only the QS measurements from microphones 2, 3 and 4 (at the same heights of the microphones on the Adrienne grid) where analyzed and 3 consecutive measurements spaced laterally by 0.4 m were performed, to *virtually* measure at all the 9 microphone positions of the Adrienne grid.

The measurements were made on a noise barrier made of perforated metal cassettes, filled with sound absorbing polyester fiber, as shown in Figure 17. In both cases the

lightweight loudspeaker was used, as its time and frequency responses are comparable to those of the Zircon system (Figure 15 and Figure 16).

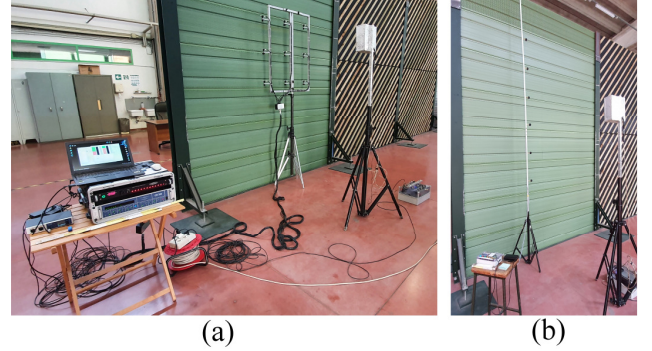


**Figure 17.** Measurements on the same noise barrier with (a) the Adrienne System and (b) the Quick System.

### A. Sound reflection index measurements

Figure 18 shows the comparison between the average reflection index, in third-octave bands, measured with the Adrienne system and the microphone grid and with the Quick System and the virtual grid described above; see formula (1). It can be seen that the two plots are practically identical at all frequencies.

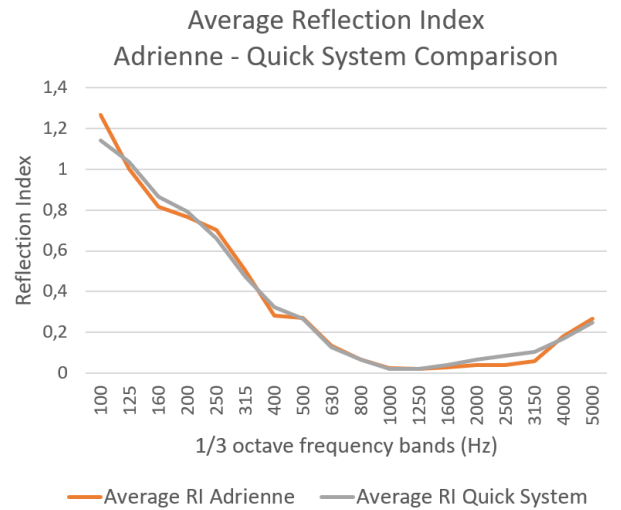


**Figure 18.** Comparison of the sound reflection index, averaged on 9 microphone positions, measured with the Adrienne System and the Quick System.

Table 1 reports the single-number ratings  $DL_{RI}$  [1] calculated from the Adrienne and Quick System measurements in the frequency range 200 Hz to 5 kHz. A small difference of 0.1 dB can be observed, well below the expanded uncertainty of 1.4 dB at 95% confidence derived from the inter-laboratory test [42], confirming that the QS works very well for sound reflection index measurements.

### B. Sound insulation index measurements

Figure 19 shows the comparison between the average sound insulation index, in third-octave bands, measured with the Adrienne system and the microphone grid and with the Quick System and the virtual grid described above; see formula (2). Also in this case, a good overlap of the measurements made with the two systems can be observed.

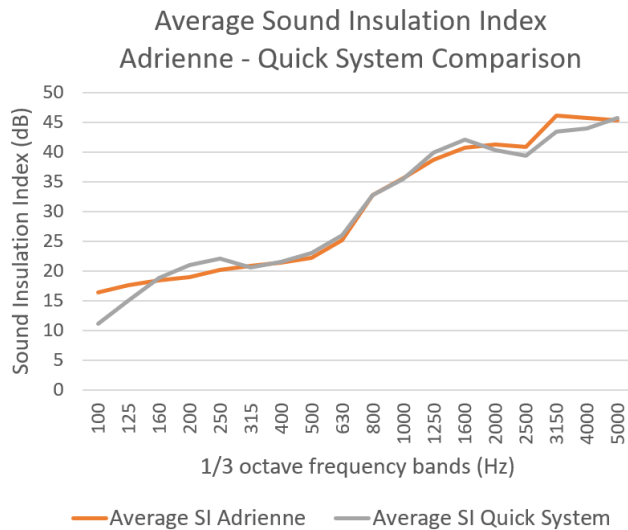


**Figure 19.** Comparison of the sound insulation index, averaged on 9 microphone positions, measured with the Adrienne System and the Quick System.

Table 1 reports the single-number ratings  $DL_{SI}$  [2] calculated from the Adrienne and Quick System measurements in the frequency range 200 Hz to 5 kHz. A small difference of - 0.7 dB can be observed, well below the expanded uncertainty of 2.1 dB at 95% confidence derived from the inter-laboratory test [42], confirming that the QS works very well also for sound insulation index measurements.

**Table 1.** single-number ratings of the sound reflection index and the sound insulation index, averaged on 9 microphone positions, measured with the Adrienne System and the Quick System in the range 200 Hz to 5 kHz, in one-third octave bands.

	Adrienne system	Quick system
$DL_{RI}$ , dB	8.6	8.5
$DL_{SI}$ , dB	26.9	27.6

### C. Signal to Noise ratio

The MLS signal, for both the Adrienne and Quick System measurements, was 262143 samples long, at a sampling frequency of 44.1 kHz, corresponding to a duration of 5.944 seconds and had a total pressure level of about 85 dB. This level, with the loudspeaker used, allows a good value of the signal-to-noise ratio (SNR) in the measurements and at the same time maintains a low distortion of the loudspeaker, which was observed in the total lack of spurious spikes spread along

the time axis of the impulse responses, whose presence would be a symptom of distortion [35]-[36]. The measurements in the laboratory took place in a reasonably quiet environment, with some normal background noise from people working nearby. Due to the well-known property of the MLS method for measuring impulse responses, background noise was mostly rejected from the measured impulse responses.

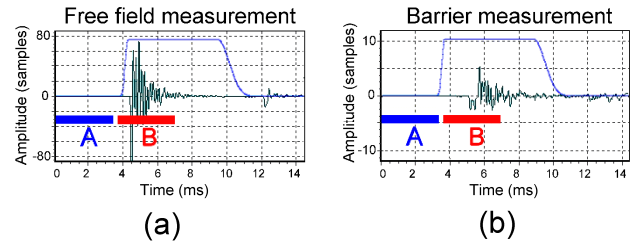


**Figure 20.** Selection of time data for SNR computation from impulse responses taken in a sound insulation measurement on a poorly insulating barrier. (a) Free-field measurement; (b) across barrier measurement. A: background noise part; B: signal part.

The actual signal-to-noise ratio in the MLS-measured impulse response is calculated by the Adrienne and Quick System software by windowing a 3.5 ms portion of time data in the zone of the highest impulse energy (time interval B in figure 20,) and a 3.5 ms portion of time data in the initial zone of the impulse response, before the sound arrives at the microphone, which therefore contains only the noise floor of the measurement (time interval A in figure 20). The ratio of the power spectra of these two portions of data yields the signal-to-noise ratio for each 1/3-octave band, as described in detail in [43]. The time length of the data windows of 3.5 ms allows a valid frequency analysis from the 400 Hz band to 5 kHz. From the difference of the total RMS power of the signal and of the noise floor, the SNR is calculated.

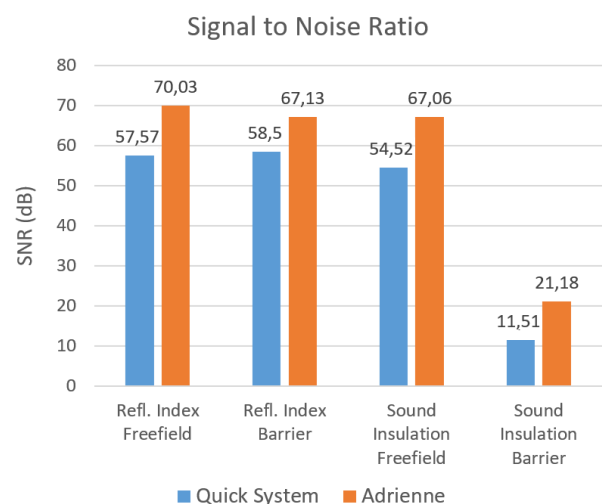


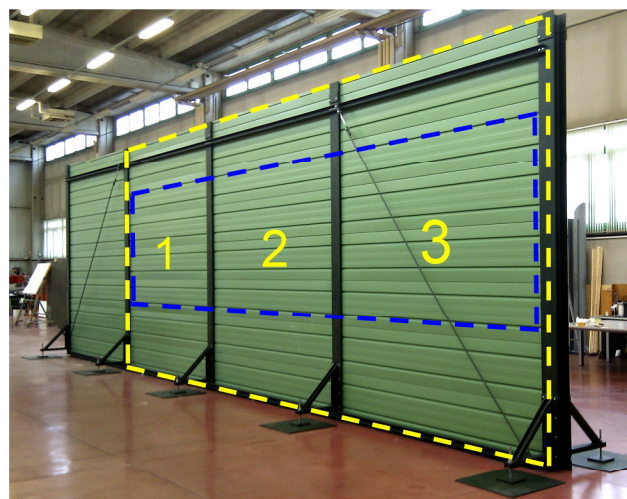
**Figure 21.** SNR obtained in the comparison measurements between the Adrienne system and the Quick system.



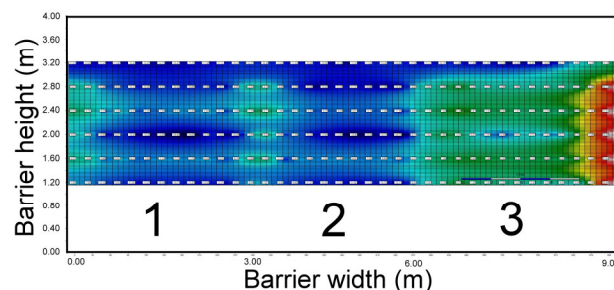
The values shown in Figure 21 were calculated from the impulse responses measured at the microphone on axis with the loudspeaker (similar values are found for the other microphones). It can be seen that for the reflection index measurements, the SNRs for the free-field and barrier measurements are similar, considering each measurement system. For the sound insulation index measurement, the value from the barrier measurement is low, as expected, since the impulse response is measured behind the barrier, thus at a much lower level. It can be seen that the Quick System has SNR values about 10 dB lower than those of the Adrienne system. This is due to the use of low-cost components (especially the electret microphones versus the Piezotronics PCB model 130F20 used with the Adrienne system) and for the 16-bit sampling of the QS versus the 24-bit sampling of the Adrienne system, which employs an expensive, high-precision, recording studio level A/D converter. In spite of these differences, the Quick System presents very good SNR values, certainly sufficient to perform the measurements correctly.

#### D. Example of extensive barrier surface analysis

One of the main improvements of the Quick System over the Adrienne system is the capability of testing a larger portion of the barrier surface thanks to the linear antenna. The microphones of the antenna at height above ground 1.60 m, 2.00 m and 2.40 m are at the same height as microphones on the Adrienne grid. In addition, a lower microphone at 1.20 m and two higher ones at 2.80 m and 3.20 m are placed. Displacing the antenna in small horizontal steps and repeating the measurement – possible within a short time with the QS - a larger portion of the barrier can be analysed, providing detailed information on possible manufacturing or installation defects. If necessary, the 3 microphones at the same height as the Adrienne grid make it possible, by taking 3 measurements horizontally spaced 40 cm apart, to virtually reconstruct the Adrienne grid and obtain completely equivalent results. An example of detailed analysis is shown in Figure 22, which represents a barrier insulation survey, carried out with the linear antenna, on the barrier fields 1, 2 and 3 and on the two intermediate posts (area outlined in yellow), moving the antenna and the loudspeaker at a horizontal step of 25 cm. The 6 microphones of the antenna allow the area outlined in blue to be analysed in detail (the upper and lower parts cannot be tested with this method for physical reasons, i.e. proximity to the open top edge of the barrier and the presence of sound reflections on the ground, respectively). Although the barrier externally appears to be uniform, the rightmost element, marked with the number 3, contains a lower density material and consequently has less sound insulation, as is clearly shown in the interpolated plot of power spectra behind the barrier, relative to the 1/3 octave band of 630 Hz. There is also a noticeable insulation leak in the central part of panel 3 (blue spot), which could result from an installation defect or inhomogeneity of the filling material. By normalising these spectra against reference free-field responses, the insulation coefficients can be obtained. More details on this measurement are given in [46].



(a)



(b)

**Figure 22.** Investigation in search of insulation leaks on the entire surface of the barrier. (a) Analysed portion of the barrier (outlined area in yellow) and portion covered by the microphone antenna (outlined area in blue); (b) interpolated punctual power spectrum.

### IX. HIGHLIGHTS OF THE QUICK SYSTEM

#### A. Main benefits

- A1) in situ measurement easier and faster than with the Adrienne system
- A2) measurement over a an area of the noise barrier much larger than with the Adrienne system
- A3) measurement results comparable to those of the Adrienne system, or identical if necessary, using the virtual grid method, as shown in the comparison in Section VIII

#### B. Additional benefits

- B1) fast on-site setup and quick measurement execution
- B2) low cost
- B3) lightweight
- B4) long battery operation time
- B5) wireless loudspeaker connection

### X. CONCLUSION AND OUTLOOK

A new Quick System for fast measurements of the acoustic intrinsic characteristics of noise barriers has been presented.

The design and implementation of the system has been described; each part of the system has been validated vs the standard Adrienne system already in use since several years for checking installed noise barriers according to European standards EN 1793-5 and EN1793-6. The new QS allows fast sound reflection index and sound insulation measurements to be carried out on noise barriers installed along motorways and railways with a lightweight and easy-to-use instrumentation and an autonomy of several working days. The new system performs automated measurements pushing few buttons, so that non-expert operators can use it routinely. The availability of such quick measurement systems paves the way to the inspection of a greater part of installed noise barriers, both for finding possible defects and then decide on maintenance actions and to assess the variability of real-life noise barriers along their entire length. The new QS opens these possibilities for the first time, but to give a solid basis to them a statistical investigation should be done to assess the correct sample size to draw reliable conclusions. This new research has been already started and will be reported in a forthcoming work.

*Work done in the frame of the SOPRANOISE project, funded by CEDR (Conference of European Directors of Roads) as a part of their Transnational Road Research Program, Call 2018.*

## REFERENCES

- [1] EN 1793-5:2016/AC:2018 Road traffic noise reducing devices - Test method for determining the acoustic performance - Part 5: Intrinsic characteristics - In situ values of sound reflection under direct sound field conditions.
- [2] EN 1793-6:2018/A1:2021: Road traffic noise reducing devices - Test method for determining the acoustic performance - Part 6: Intrinsic characteristics - In situ values of airborne sound insulation under direct sound field conditions.
- [3] J. Huang, C. Lee, C. Yeh, W. Wu, C. Lin, "High-Precision Ultrasonic Ranging System Platform Based on Peak-Detected Self-Interference Technique", *IEEE Trans. Instrum. Meas.*, vol. 60, no. 12, pp. 3775-3780, Dec. 2011.
- [4] G. Quintero, A. Balastegui, J. Romeu, "A low-cost noise measurement device for noise mapping based on mobile sampling", *Measurement*, vol. 148, Article 106894, Dec. 2019.
- [5] R. A. D. Esmeralda, R. J. A. Regalado, G. I. J. F. Rosa, R. S. Pangantihon, "Automated Hollow Tile Floor Detector Using Fast Fourier Transform", *2019 IEEE 11th International Conference on Humanoid, Nanotechnology, Information Technology, Communication and Control, Environment, and Management (HNICEM)*, pp. 1-5, 2019.
- [6] W. D. Fonseca, F. R. d. Mello, D. R. Carvalho, P. H. Mareze, O. M. Silva, "Measurement of car cabin binaural impulse responses and auralization via convolution", *2021 Immersive and 3D Audio: from Architecture to Automotive (I3DA)*, pp. 1-13, 2021.
- [7] P. R. Leary, V. N. Dobrokhodov, K. D. Jones and K. B. Smith, "Real-Time Multi-Channel Acoustic Beamforming Using a Lightweight Microcontroller Processor", *OCEANS 2019 MTS/IEEE SEATTLE*, pp. 1-6, 2019.
- [8] S. Paul, S. Mulani, N. Daimary, M. S. Singh, "Simplified-Delay-Multiply-and-Sum-Based Promising Beamformer for Real-Time Photoacoustic Imaging", *IEEE Trans. Instrum. Meas.*, vol. 71, pp. 1-9, 2022.
- [9] Z. Sheng, S. Pfersich, A. Eldridge, J. Zhou, D. Tian and V. C. M. Leung, "Wireless acoustic sensor networks and edge computing for rapid acoustic monitoring", in *IEEE/CAA Journal of Automatica Sinica*, vol. 6, no. 1, pp. 64-74, January 2019.
- [10] V. Bianchi, A. Boni, S. Fortunati, M. Giannetto, M. Careri, I. De Munari, "A Wi-Fi Cloud-Based Portable Potentiostat for Electrochemical Biosensors", *IEEE Trans. Instrum. Meas.*, vol. 69, no. 6, pp. 3232-3240, June 2020.
- [11] M. Schmidt, D. Penner, A. Burkl, R. Stojanovic, T. Schümann, P. Beckerle, "Implementation and evaluation of a low-cost and compact electrodermal activity measurement system", *Measurement*, vol. 92, pp. 96-102, 2016.
- [12] L. E. Sebar, L. Iannucci, E. Angelini, S. Grassini, M. Parvis, "Electrochemical Impedance Spectroscopy System Based on a Teensy Board", *IEEE Trans. Instrum. Meas.*, vol. 70, pp. 1-9, 2021.
- [13] C. N. Murthy, S. Ramagopal, S. Asokan, "A simple low-cost electrical switching analyzer for I-V characterization of switching samples and devices", *IEEE Trans. Instrum. Meas.*, vol. 55, no. 1, pp. 248-256, Feb. 2006.
- [14] R. Mulla, K. Glover, C. W. Dunnill, "An Easily Constructed and Inexpensive Tool to Evaluate the Seebeck Coefficient", *IEEE Trans. Instrum. Meas.*, vol. 70, pp. 1-7, 2021.
- [15] Y. H. Tehrani, S. M. Atarodi, "Design & Implementation of High Dynamic Range Current Measurement System for IoT Applications", *IEEE Trans. Instrum. Meas.*, vol. 71, pp. 1-9, 2022.
- [16] H. Katdare, N. Warke, P. Vaidya, "Design and Construction of Low Cost High-Performance Transducer Signal Processing and Data Acquisition System", *2020 4th International Conference on Trends in Electronics and Informatics (ICOEI)*(48184), pp. 48-52, 2020.
- [17] S. Singh, S. K. Pandey, "Fabrication of Simple Apparatus for Resistivity Measurement in High-Temperature Range 300–620 K", *IEEE Trans. Instrum. Meas.*, vol. 67, no. 9, pp. 2169-2176, Sept. 2018.
- [18] F. Reverter, Ò. Casas, "Interfacing Differential Resistive Sensors to Microcontrollers: A Direct Approach", *IEEE Trans. Instrum. Meas.*, vol. 58, no. 10, pp. 3405-3410, Oct. 2009.
- [19] N. Gunawardena, E. R. Pardyjak, R. Stoll, A. Khadka, "Development and evaluation of an open-source, low-cost distributed sensor network for environmental monitoring applications", *Meas. Sci. Technol.*, vol. 29, no. 2, January 2018.
- [20] J. Pelegri-Sebastia, E. Garcia-Breijo, J. Ibanez, T. Sogorb, N. Laguarda-Miro, J. Garrigues, "Low-Cost Capacitive Humidity Sensor for Application Within Flexible RFID Labels Based on Microcontroller Systems", *IEEE Trans. Instrum. Meas.*, vol. 61, no. 2, pp. 545-553, Feb. 2012.
- [21] Y. Ye, S. Wan, S. Li, X. He, "Mechanical Wind Sensor Based on Additive Manufacturing Technology", *IEEE Trans. Instrum. Meas.*, vol. 71, pp. 1-8, 2022.
- [22] D. Trebbels, A. Kern, F. Fellhauer, C. Huebner, R. Zengerle, "Miniaturized FPGA-Based High-Resolution Time-Domain Reflectometer", *IEEE Trans. Instrum. Meas.*, vol. 62, no. 7, pp. 2101-2113, July 2013.
- [23] L. Zhang, F. Tian, "Performance Study of Multilayer Perceptrons in a Low-Cost Electronic Nose", *IEEE Trans. Instrum. Meas.*, vol. 63, no. 7, pp. 1670-1679, July 2014.
- [24] L. K. Baghel, S. Gautam, V. K. Malav, S. Kumar, "TEMPSENSE: LoRa Enabled Integrated Sensing and Localization Solution for Water Quality Monitoring", *IEEE Trans. Instrum. Meas.*, vol. 71, pp. 1-11, 2022.
- [25] P. Arpaia, U. Cesaro, N. Moccaldi, "A Bioimpedance Meter to Measure Drug in Transdermal Delivery", *IEEE Trans. Instrum. Meas.*, vol. 67, no. 10, pp. 2324-2331, Oct. 2018.
- [26] A. Bergeron, N. Baddour, "Design and Development of a Low-Cost Multisensor Inertial Data Acquisition System for Sailing", *IEEE Trans. Instrum. Meas.*, vol. 63, no. 2, pp. 441-449, Feb. 2014.
- [27] E. Taylor, J. Bonner, R. Nelson, C. Fuller, W. Kirkey, S. Cappelli, "Development of an in-situ total phosphorus analyzer", *OCEANS 2015 - MTS/IEEE Washington*, pp. 1-4, 2015.
- [28] C. Saputra, M. M. Munir, A. Waris, "Digital pulse analyzer for simultaneous measurement of pulse height, pulse width, and interval time on an optical particle counter", *Meas. Sci. Technol.*, vol. 31, no. 6, March 2020.
- [29] J. Huang, T. Zhou, H. Liu, L. Qi, Y. Liu, Y. Li, "Low-Noise, High-Linearity Sine-Wave Generation Using Noise-Shaping Phase-Switching Technique", *IEEE Trans. Instrum. Meas.*, vol. 71, pp. 1-7, 2022.
- [30] M. B. de Moraes França, F. J. O. Moraes, P. Carvalhaes-Dias, L. C. Duarte, J. A. Siqueira Dias, "A Multiprobe Heat Pulse Sensor for Soil Moisture Measurement Based on PCB Technology", *IEEE Trans. Instrum. Meas.*, vol. 68, no. 2, pp. 606-613, Feb. 2019.
- [31] I. Al-Bahadly, J. Thompson, "Garden watering system based on moisture sensing", *2015 9th International Conference on Sensing Technology (ICST)*, pp. 263-268, 2015.
- [32] R. B. de Freitas, V. N. H. Silva, V. T. Maia, O. B. d. Santos, Y. M. de Arruda Calvete, S. B. Fiaux, "Low-Cost Device to Measure Concentration of *Saccharomyces cerevisiae* Through Methylene Blue Reduction", *IEEE Trans. Instrum. Meas.*, vol. 69, no. 5, pp. 2232-2238, May 2020.
- [33] J. Borish, J. B. Angell, "An efficient algorithm for measuring the impulse response using pseudorandom noise", *J. Audio Eng. Soc.*, vol. 31, no. 7/8, pp. 478-488, 1983.
- [34] D. D. Rife, J. Vanderkooy, "Transfer-function measurement with maximum-length sequences", *J. Audio Eng. Soc.*, vol. 37, no. 6, pp. 419-444, 1989.
- [35] D. D. Rife, "Modulation Transfer Function Measurement with Maximum Length Sequences", *J. Audio Eng. Soc.*, vol. 40, no. 10, pp. 779-790, 1992.
- [36] M. Vorländer, M. Kob, "Practical aspects of MLS measurements in

building acoustics”, *Appl. Acoust.*, vol. 54, no. 3-4, pp. 239-258, 1997.

[37] G. Stan, J.J. Embrechts, D. Archambeau, “Comparison of Different Impulse Response Measurement Techniques”, *J. Audio Eng. Soc.*, vol. 50, no. 4, pp. 249-262, 2002.

[38] D. Ćirić, “Comparison of influence of distortion in MLS and Sine Sweep technique”, in *19th International Congress on Acoustics*, paper RBA-07-020, September 2007.

[39] J. Borish, J. B. Angell, “An efficient algorithm for measuring the impulse response using pseudorandom noise”, *J. Audio Eng. Soc.*, vol. 31, no. 7/8, pp. 478-488, 1983.

[40] Y. Ando, *Concert Hall Acoustics*. Springer series in Electrophysics, vol 17, Springer-Verlag, Berlin Heidelberg, 1985.

[41] P. Robinson, N. Xiang, “On the subtraction method for in-situ reflection and diffusion coefficient measurements”, *J. Acoust. Soc. Am.*, vol. 127, no. 3, EL99, 2010.

[42] M. Garai, P. Guidorzi et al., “Repeatability and reproducibility of in situ measurements of sound reflection and airborne sound insulation index of noise barriers”, *Acta Ac. united with Acustica*, vol 100, no. 6, pp.1186-1201, 2014.

[43] P. Guidorzi, M. Garai, “Impulse responses measured with MLS or Swept-sine signals: A comparison between the two methods applied to noise barriers measurements”, in *Proceedings of the 134th Audio Engineering Society Convention*, Rome, Italy, 2013.

[44] M. Garai, P. Guidorzi, “Sound reflection measurements on noise barriers in critical conditions”, *Build. Environ.*, vol. 94, no. 2, pp. 752-763, 2015.

[45] P. Guidorzi, M. Garai, “Signal analysis in the sound absorption measurement procedure: The importance of time subtraction and reference surface corrections”, in *Proc. Acoustics-08*, Paris, 29 June-4 July, 2008.

[46] P. Guidorzi, M. Garai, “Sound insulation measurements on noise barriers across their entire extension: a preliminary study”, in *Proceedings of 2020 International Congress on Noise Control Engineering, INTER-NOISE 2020*, 23 August 2020, Seoul, 2020.

[47] *Teensyduino programming tool*. Accessed: Jul. 20, 2022. [Online]. Available: <https://www.pjrc.com/teensy/teensyduino.html>

[48] *Audio System Design Tool for Teensy Audio Library*. Accessed: Jul. 20, 2022. [Online]. Available: <https://www.pjrc.com/teensy/gui/index.html>

[49] R. Michon, Y. Orlarey, S. Letz, and D. Fober, “Real Time Audio Digital Signal Processing with Faust and the Teensy”, in *Proceedings of the Sound and Music Computing Conference (SMC-19)*, Malaga, Spain, 2019.

[50] L. Hallett, M. Tatum, G. Thomas, S. Sousan, K. Koehler, T. Peters, “An inexpensive sensor for noise”, *J. Occup. Environ. Hyg.*, vol. 15, no. 5, pp. 448-454, 2018.

barrier for roads and railways, room and building acoustics, environmental sustainability.



**Paolo Guidorzi** was born in Italy in 1969. He received his MS degree in Electrical Engineering and PhD in Applied Acoustics from the University of Bologna, Italy, in 1995 and 1999, respectively. He is currently an Assistant Professor at the Department of Industrial Engineering, School of Engineering, University of

Bologna. His main research fields are noise barrier measurement, signal processing, development of hardware and software for acoustic measurement instruments, acoustic measurements.



**Massimo Garai**, was born in Italy in 1959. He received his MS degree in Physics and PhD in Applied Acoustics from the University of Bologna, Italy, in 1983 and 1991, respectively. He is currently a full-time Professor at the Department of Industrial Engineering, University of Bologna. He is president of the Italian Committee for Acoustics and Vibration at

the National standard body (UNI). His main research fields are acoustic metamaterials, machine learning in acoustics, noise